Photoluminescence and energy transfer studies of $YAl_3(BO_3)_4:Sm^{3+}/Tb^{3+}$ phosphors for solid state lighting applications

G. V. LOKESWARA REDDY[a], L. RAMA MOORTHY[a,b], K. PAVANI[a], B. C. JAMALAIAH[a,c*]
[a]*Department of Physics, Sri Venkateswara University, Tirupati 517 502, India*
[b]*Department of Physics, Chadalawada Venkata Subbaiah Engineering College, Tirupati 517 506, India*
[c]*Department of Materials Engineering and Ceramics, CICECO, University of Aveiro, Campus Santiago, 3810-193 Aveiro, Portugal*

Trivalent samarium (Sm^{3+})/ terbium (Tb^{3+}) co-doped $YAl_3(BO_3)_4$ (YAB) phosphors were prepared by solid-state reaction method. The phase, structure, optical and energy transfer studies were systematically characterized through X- ray diffraction, Fourier transform infrared spectroscopy, photoluminescence (PL) and decay measurements, respectively. Upon 406 nm excitation, both Sm^{3+} single- and Sm^{3+}/Tb^{3+} co-doped YAB phosphors emit orange-red luminescence with peak maximum at 602 nm. The YAB:Tb^{3+} phosphor emits green luminescence at 546 nm when excited with 375 nm near UV wavelength. The YAB:Sm^{3+}/Tb^{3+} phosphors emit green-to-white luminescence as a function of Sm^{3+} concentration upon an excitation wavelength of 375 nm. The Tb^{3+} acts as an efficient sensitizer of luminescence of Sm^{3+} under 375 nm excitation in YAB phosphors. Doped Sm^{3+} and Tb^{3+} ions were located at the inversion symmetry sites of YAB lattice. The Commission International de l'Eclairage chromaticity coordinates were calculated from the PL spectra. The energy transfer from Tb^{3+} to Sm^{3+} ions was described in detail. The YAB:Sm^{3+}/Tb^{3+} phosphors can be used as a promising material for solid state lighting devices.

(Received June 25, 2013; accepted September 18, 2013)

Keywords: Yttrium-borate phosphors, Photoluminescence, Energy transfer, Solid state lighting

1. Introduction

Recently, the synthesis and characterization of oxide based nanocrystalline phosphors has become a fascinating field of research for white light-emitting diodes and field emission display devices due to their stable and environmental friendly behaviour [1,2]. Trivalent rare earth (RE^{3+}) ions have been playing a significant role in modern solid state lighting (SSL) applications due to their rich emission colours related to the 4f → 4f transitions. Moreover, the host matrix has little influence on the positions of 4f configuration energy levels, which are almost the similar as that of the free-ion levels. Among the available yttrium-borate based phosphors, the $YAl_3(BO_3)_4$ (YAB) phosphor has been used as a promising candidate for host lattice for various photonic device applications due to its wide isomorphous substitutions, ultra violet (UV) transparency and non-linear optical properties [3-5]. The YAB crystal lattice belongs to the mineral huntite $CaMg_3(CO_3)_4$ type structure of space group R32 with Y-centered distorted trigonal prisms and Al-centered distorted octahedral dispersed between planes of BO_3 triangles [6].

Generally, RE^{3+} ions have been considered as the most important optical activators for luminescent devices. Among the RE ions, the Sm^{3+} ion emits orange-red luminescence due to the $^4G_{5/2} \rightarrow {}^6H_{5/2,7/2,9/2}$ transitions and acts as an excellent activator with high luminescence output, colour purity and thermal stability [7,8]. On the other hand, the Tb^{3+} ions emits green luminescence corresponding to the $^5D_4 \rightarrow {}^7F_J$ (J = 6,5,4,3) transitions at higher concentrations (≥ 0.5%) and blue luminescence related to the $^5D_3 \rightarrow {}^7F_J$ transitions at lower concentrations (< 0.5%) under suitable near UV excitation besides acting as a sensitizer. However, the emission colour not only depends upon the concentration of Tb^{3+} ions but also on the phonon energy of the host lattice [9]. As per our knowledge concerned, there are no reports on the optical characterization of Sm^{3+}/Tb^{3+} co-doped YAB phosphors. Hence, we present the structural and optical characterization of YAB:Sm^{3+}/Tb^{3+} phosphors prepared by solid-state reaction method. The luminescence decay analysis of Sm^{3+}:$^4G_{5/2}$ and Tb^{3+}:$^5D_4$ emission states and the energy transfer (ET) from Tb^{3+} to Sm^{3+} ions are also discussed in detail. These phosphors have potential applications in SSL which uses LEDs for illumination.

2. Experimental

2.1. Materials and method

High-purity Y_2O_3 (99.99%), Al_2O_3 (99.9%), H_3BO_3 (99.5%), Sm_2O_3 (99.99%) and Tb_4O_7 (99.99%) from Sigma-Aldrich were taken as the starting chemicals. The YAB:Sm^{3+}/Tb^{3+} phosphors of chemical formula,

$Y_{(1-x-y)}Al_3(BO_3)_4:xSm^{3+}/yTb^{3+}$ (x = 0, 0.3, 0.5, 1.0, 2.0% and y = 0.5%) phosphors were prepared by solid-state reaction method. The starting chemicals were grinded homogeneously in the presence of acetone using a pestle and an agate mortar. An excess of 3% of H_3BO_3 was added to compensate its evaporation while heating. The samples were fired at 200 and 600°C for 3h and finally sintered at 1200°C for 3h in CO atmosphere using alumina crucible.

2.2. Characterization

The X-ray diffraction (XRD) measurements were carried out on X'Pert- Pro Materials Research Diffractometer using CuKα radiation of λ = 1.5406 Å. The Fourier transform infrared (FTIR) spectra were recorded using Thermo Nicolet IR200 spectrophotometer. The photoluminescence excitation, emission and luminescence decay measurements were performed on a Jobin YVON Fluorolog-3 spectrofluorimeter. All the measurements were carried out at room temperature only.

3. Results and discussion

3.1. XRD and FTIR analysis

The XRD patterns of undoped, Sm^{3+}-, Tb^{3+}- and Sm^{3+}/Tb^{3+} co-doped YAB phosphors shown in Fig. 1a are suitably matched with the JCPDS Card No. 72-1978. The decrease in intensity of XRD peaks with the increase of dopant concentration, reveal that the Sm^{3+} and Tb^{3+} ions suitably replace the Y^{3+} sites without disturbing the YAB crystal lattice due to their chemical valences and ionic radii (Y^{3+}: 0.090 nm; Sm^{3+}: 0.096 nm; Tb^{3+}: 0.092 nm). However, the peak positions remain unchanged. Apart from the YAB phase, YBO_3 phase is also appeared in XRD patterns which might be due to boron loss at higher temperatures or the slower reaction rate of Al_2O_3 with Y_2O_3 and B_2O_3 [10,11]. Further, the YBO_3 phase which is almost negligible when compared to the YAB phase does not influence the optical transitions of RE ions [3].

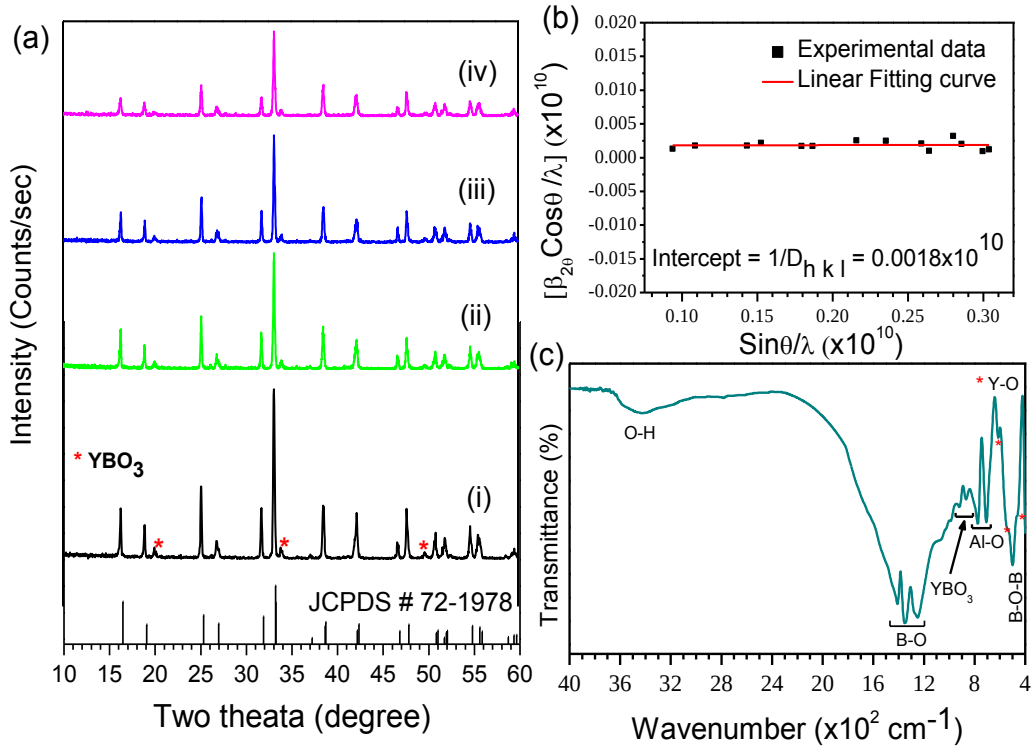

Fig. 1. XRD profiles of (i) undoped, (ii) 0.5%Tb^{3+}, (iii) 1%Sm^{3+}, (iv) 2%Sm^{3+}/0.5%Tb^{3+} -doped YAB phosphors (a), the Hall-Williamson plot for YAB:2%Sm^{3+}/0.5%Tb^{3+} phosphor (b) and the FTIR spectrum for YAB phosphor (c).

The average size of crystallites (D_{hkl}) of $YAB:Sm^{3+}/Tb^{3+}$ phosphors has been determined following the Scherrer's formula [12] and the Hall-Williamsons equation [13]:

$$D_{hkl} = \frac{0.89\,\lambda}{\beta_{2\theta}\,Cos\theta} \quad \text{(Scherrer's formula)} \quad (1)$$

$$\frac{\beta_{2\theta}\,Cos\theta}{\lambda} = \frac{1}{D_{hkl}} + \frac{\varepsilon\,Sin\theta}{\lambda} \quad \text{(Hall-Williamsons equation)} \quad (2)$$

where λ is the wavelength of X-rays (1.5406 Å), $\beta_{2\theta}$ is the full width at half maximum, θ is the angle of diffraction, and ε is the micro-strain present in the given phosphor. The average crystallite size of the $YAB:Sm^{3+}/Tb^{3+}$ phosphors is determined to be ~54 nm from the Scherrer's formula. It can also be calculated from ($\beta_{2\theta}$ Cosθ)/λ versus Sinθ/λ plot following the Hall-Williamsons method. Fig. 1b presents the ($\beta_{2\theta}$Cosθ)/λ versus Sinθ/λ plot for $YAB:2\%Sm^{3+}/0.5\%Tb^{3+}$ phosphor.

The reciprocal of the intercept of its straight plot indicates the average crystallite size of ~55 nm which is very close to that estimated from the Scherrer's formula.

The FTIR spectrum for YAB host phosphor is illustrated in Fig. 1c. The IR absorption bands have been attributed to OH (3428.82 cm^{-1}), B-O asymmetric stretching vibration (1413.63 cm^{-1}), B-O stretching vibration (1354.72 and 1251.65 cm^{-1}), B-O-B bending vibration (499.75 cm^{-1}) Al-O stretching vibration (775.53 and 706.81 cm^{-1}) and Y-O stretching vibration (613.54, 541.90 and 461.38 cm^{-1}) [14-17]. The weak IR absorption bands located at ~1064.53, ~917.67 and ~868.79 cm^{-1} could be due to the YBO_3 phase [11,18]. From the literature [19], it is well known that the OH content increases the optical losses and then decrease the luminescence efficiency of RE ions. As seen the FTIR spectrum, the IR absorption band related to OH group is very weak and it does not affect the optical transitions of RE ions present in the YAB phosphor.

3.2. Photoluminescence of Sm^{3+} and Sm^{3+}/Tb^{3+} phosphors

The photoluminescence excitation (PLE) spectrum of YAB:1%Sm^{3+} phosphor by monitoring the emission at 602 nm corresponding to the $^4G_{5/2} \rightarrow {}^6H_{7/2}$ transition of Sm^{3+} ion is shown in Fig. 2a. This figure is composed of a series of PLE bands centered at 319, 334, 348, 364, 380, 392, 406, 423, 467, 478 and 488 nm corresponding to the $^6H_{5/2} \rightarrow {}^4G_{11/2}$, $^4G_{7/2}$, $^4K_{15/2}$, $^4F_{9/2}$, $^4D_{1/2}$, $^4L_{15/2}$, $^4L_{13/2}$, $^4M_{19/2}$, $^4I_{13/2}$, $^4I_{11/2}$, $^4I_{9/2}$ transitions, respectively [20]. The PLE spectra of YAB:*x*Sm^{3+}/0.5%Tb^{3+} phosphors exhibit similar spectral features under the same experimental conditions and the PLE spectrum of YAB:2%Sm^{3+}/0.5%Tb^{3+} phosphor is presented in Fig. 2a (as a reference). In Sm^{3+}/Tb^{3+} co-activated phosphors, the intensity of observed PLE bands of Sm^{3+} increases with the increase of its concentration which means the uniform distribution of Sm^{3+} and Tb^{3+} ions in YAB phosphors. The variation of intensity of Sm^{3+}:$^6H_{5/2} \rightarrow {}^4L_{13/2}$ transition is shown in Fig. 2b. As seen the PLE spectrum of YAB:2%Sm^{3+}/ 0.5%Tb^{3+} phosphor, one can notice the non-existence of PLE bands of Tb^{3+} ion when the major emission of Sm^{3+} ion through the $^4G_{5/2} \rightarrow {}^6H_{7/2}$ transition is monitored indicates the absence of energy transfer (ET) from Sm^{3+} to Tb^{3+} ions. Among the observed PLE transitions, the $^6H_{5/2} \rightarrow {}^4L_{13/2}$ (406 nm) transition has highest intensity and the wavelength corresponding to this transition is used to investigate the PL of Sm^{3+}/Tb^{3+} co-doped YAB phosphors.

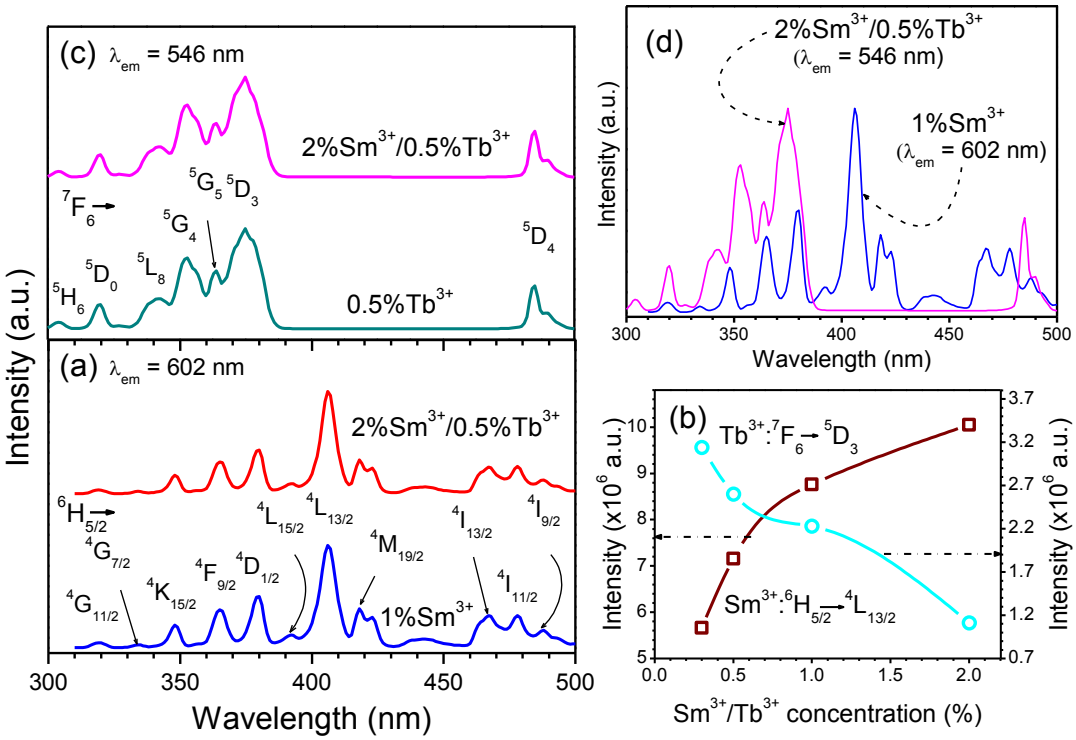

Fig. 2. PLE spectra with λ_{em} = 602 nm (a), variation of intensity as a function of Sm^{3+}/Tb^{3+} concentration (b), PLE spectra with λ_{em} = 546 nm (c) and overlapped PLE bands of Tb^{3+} and Sm^{3+} ions in Sm^{3+}- and Sm^{3+}/Tb^{3+} co-doped phosphors (d).

Upon 406 nm excitation, the PL spectra of Sm^{3+} single- and Sm^{3+}/Tb^{3+} co-doped YAB phosphors exhibit Sm^{3+} characteristic emission bands in the spectral range from 500 to 700 nm (Figs. 3a and b). The emission bands centered at 567 and 602 nm have been assigned to the $^4G_{5/2} \rightarrow {}^6H_{5/2}$ and $^4G_{5/2} \rightarrow {}^6H_{7/2}$ magnetic dipole transitions

($\Delta J = 0, \pm 1$), respectively, while the band with peak maximum at 649 nm is assigned to the $^4G_{5/2} \rightarrow {}^6H_{9/2}$ electric dipole transition ($\Delta J \leq 6$) [21]. Among these, the emission at 602 nm associated with the $^4G_{5/2} \rightarrow {}^6H_{7/2}$ transition is found to be intense. The partial energy level diagram shown in Fig. 4 describes the emission mechanism of Sm^{3+} ion in YAB phosphors. As seen the PL spectra of Sm^{3+}/Tb^{3+} co-activated YAB phosphors, the luminescence intensity increases with the increase of Sm^{3+} concentration up to 1% and then decreases for further increase of its concentration owing to the phenomenon of luminescence quenching in RE ions. Since there is no ET from Sm^{3+} to Tb^{3+}, the luminescence quenching could be due to the interaction of excited Sm^{3+} ions at higher concentrations. The variation of luminescence intensity of $^4G_{5/2} \rightarrow {}^6H_{7/2}$ transition with Sm^{3+}/Tb^{3+} concentration in YAB:*x*Sm^{3+}/0.5%Tb^{3+} phosphors is shown in Fig. 3c.

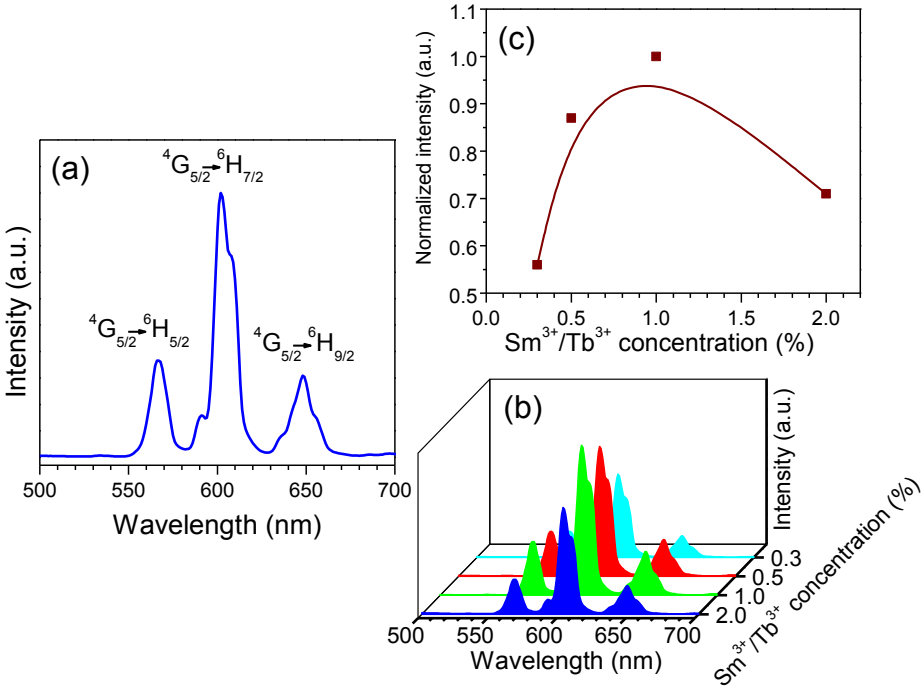

Fig.3. PL spectra for YAB:1%Sm^{3+} (a) and YAB:Sm^{3+}/Tb^{3+} (b) phosphors. The variation of intensity of $^4G_{5/2} \rightarrow {}^6H_{7/2}$ transition as a function of Sm^{3+}/Tb^{3+} concentration (c).

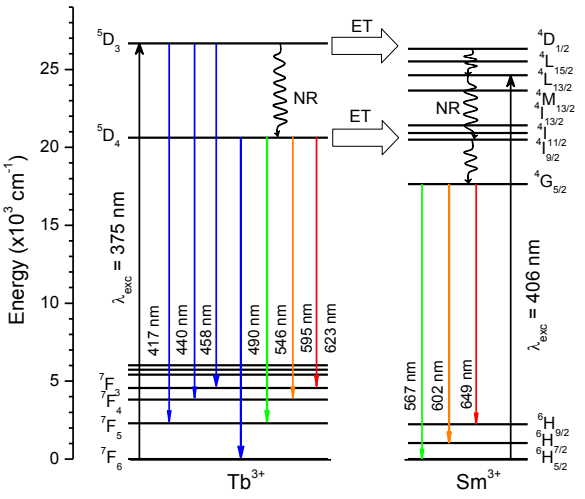

Fig. 4. Partial energy level diagram showing the emission and energy transfer mechanism in YAB:Sm^{3+}/Tb^{3+} phosphors.

The Commission International de I'Eclairage (CIE) 1931 chromaticity coordinates (x, y) calculated from the PL spectra are documented in Table 1. All these coordinates are positioned in the orange-red region (see Fig. 5). Thus, the Sm^{3+} single- and Sm^{3+}/Tb^{3+} co-doped YAB phosphors emit orange-red luminescence with 406 nm excitation and they can be applied to the orange-red emitting display devices. The relative intensity ratio of electric dipole to magnetic dipole transitions ($^4G_{5/2} \rightarrow {}^6H_{9/2}$ / $^4G_{5/2} \rightarrow {}^6H_{7/2}$) has been used to estimate the local symmetry around the Sm^{3+} ions in which they are situated. If ($^4G_{5/2} \rightarrow {}^6H_{9/2}$ / $^4G_{5/2} \rightarrow {}^6H_{7/2}$) intensity ratio is less than unity, the Sm^{3+} ions occupy inversion symmetry sites of the host lattice and the greater the intensity ratio more is the distortion from the inversion symmetry [22]. The intensity ratios calculated from the PL spectra are presented in Table 1. Upon 406 nm excitation, the intensity ratio is nearly constant (~0.28) for 1%Sm^{3+} - doped and *x*Sm^{3+}/0.5%Tb^{3+} co-doped phosphors. The smaller and constant value of ($^4G_{5/2} \rightarrow {}^6H_{9/2}$ / $^4G_{5/2} \rightarrow {}^6H_{7/2}$)

intensity ratio indicates that the doped Sm^{3+} and Tb^{3+} ions are surrounded by the inversion symmetry sites of YAB lattice.

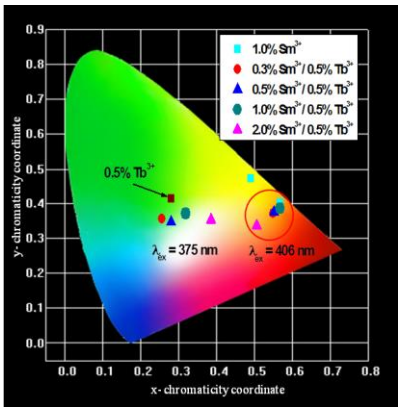

Fig. 5. (Colour online) CIE chromaticity coordinates for YAB:Sm^{3+}/Tb^{3+} phosphors.

Table 1. CIE chromaticity coordinates (x-, y-) and $\left(\frac{^4G_{5/2} \rightarrow {}^6H_{9/2}}{^4G_{5/2} \rightarrow {}^6H_{7/2}}\right)$ *intensity ratios in YAB:xSm^{3+}/0.5%Tb^{3+} phosphors under different excitation wavelengths.*

YAB phosphor doping	λ_{ex}= 406 nm			λ_{ex}= 375 nm		
	CIE coordinates		$\left(\frac{^4G_{5/2} \rightarrow {}^6H_{9/2}}{^4G_{5/2} \rightarrow {}^6H_{7/2}}\right)$	CIE coordinates		$\left(\frac{^4G_{5/2} \rightarrow {}^6H_{9/2}}{^4G_{5/2} \rightarrow {}^6H_{7/2}}\right)$
	x-	y-		x-	y-	
0.5%Tb^{3+}	-	-	-	0.238	0.418	-
1%Sm^{3+}	0.583	0.406	0.29	0.415	0.418	0.26
x = 0.3%	0.555	0.375	0.27	0.258	0.359	0.25
x = 0.5%	0.559	0.378	0.28	0.283	0.351	0.24
x = 1.0%	0.574	0.340	0.29	0.322	0.375	0.24
x = 2.0%	0.512	0.339	0.27	0.390	0.356	0.24

3.3. Photoluminescence of Tb^{3+} and Sm^{3+}/Tb^{3+} phosphors

The PLE spectrum of YAB:0.5%Tb^{3+} phosphor monitoring the emission at 546 nm is shown in Fig. 2c. This spectrum revealed seven PLE bands corresponding to the $^7F_6 \rightarrow {}^5H_6$ (304 nm), $^7F_6 \rightarrow {}^5D_0$ (320 nm), $^7F_6 \rightarrow {}^5L_8$ (342 nm), $^7F_6 \rightarrow {}^5G_4$ (353 nm), $^7F_6 \rightarrow {}^5G_5$ (364 nm), $^7F_6 \rightarrow {}^5D_3$ (375 nm) and $^7F_6 \rightarrow {}^5D_4$ (485 nm) transitions [23]. The PLE spectra of xSm^{3+}/0.5%Tb^{3+} phosphors display the similar spectral results and the PLE spectrum of YAB:2%Sm^{3+}/0.5%Tb^{3+} phosphor is illustrated in Fig. 2c (as a reference). It is noticed from Fig. 2d that some of the PLE bands of Sm^{3+} and Tb^{3+} ions overlap in the region 310-385 nm (~32260-25975 cm^{-1}) and 480-495 nm (~20830-20200 cm^{-1}). This overlap of energy levels indicates that the Tb^{3+} ion acts as a good sensitizer to the luminescence of Sm^{3+} [24]. To study the effect of sensitization of Tb^{3+} ions on the luminescence of Sm^{3+} ions, the PL measurements were carried out by exciting with 375 nm radiation. Further, the decrease in intensity of PLE transitions of Tb^{3+} ions with the increase of Sm^{3+} ions concentration is an indication of ET from Tb^{3+} to Sm^{3+}. The variation in intensity of Tb^{3+}:$^7F_6 \rightarrow {}^5D_3$ transition with Sm^{3+} concentration is also shown in Fig. 2b.

Fig. 6a describes the PL spectra of 0.5%Tb^{3+}-, 1%Sm^{3+}-, and 2%Sm^{3+}/0.5%Tb^{3+} co-doped YAB phosphors under 375 nm excitation. The PL spectrum of YAB:0.5%Tb^{3+} phosphor revealed several emission transitions both from $^5D_3$ and $^5D_4$ states in the spectral region 400-700 nm. The PL bands originating from the $^5D_3$ state are located at 417 nm ($^5D_3 \rightarrow {}^7F_5$), 440 nm ($^5D_3 \rightarrow {}^7F_4$), 458 nm and ($^5D_3 \rightarrow {}^7F_3$) and those originated from the $^5D_4$ state are centered at 490 nm ($^5D_4 \rightarrow {}^7F_6$), 546 nm ($^5D_4 \rightarrow {}^7F_5$), 595 nm ($^5D_4 \rightarrow {}^7F_4$) and 623 nm ($^5D_4 \rightarrow {}^7F_3$). Among these, the green emission at 546 nm ($^5D_4 \rightarrow {}^7F_5$) is found to be dominant. Similar results were reported for 0.07Tb^{3+}-0.07Li^+ in $Sr_2B_2O_5$ phosphor [25]. Upon 375 nm excitation, the PL spectrum of YAB:1%Sm^{3+} phosphor comprises three emission bands centered at 576 nm ($^4G_{5/2} \rightarrow {}^6H_{5/2}$), 602 nm ($^4G_{5/2} \rightarrow {}^6H_{7/2}$) and 649 nm ($^4G_{5/2} \rightarrow {}^6H_{9/2}$). These results are similar to those obtained under 406 nm excitation as seen in Fig. 3. The PL spectra (λ_{ex} = 375 nm) of YAB:xSm^{3+}/0.5%Tb^{3+} phosphors display the emission bands from both Tb^{3+} and Sm^{3+} ions. The PL spectrum of YAB:2%Sm^{3+}/0.5%Tb^{3+} phosphor is given in Fig. 6a, as a reference. The emission mechanism of Tb^{3+} and Sm^{3+} ions under 375 nm excitation is described in Fig. 4. It is quite interesting that with the increase of Sm^{3+} ion concentration, the PL intensity of

Tb^{3+} ion decreases steadily whereas the intensity of Sm^{3+} transitions increases without luminescence quenching. The variation in intensity of Tb^{3+}:$^5D_4 \rightarrow {}^7F_6$ (490 nm), Tb^{3+}:$^5D_4 \rightarrow {}^7F_5$ (546 nm) and Sm^{3+}:$^4G_{5/2} \rightarrow {}^6H_{7/2}$ (602 nm) transitions as a function of Sm^{3+}/Tb^{3+} concentration is described in Fig.6b. These results demonstrate that the Tb^{3+} ion acts as an efficient sensitizer and the YAB:Sm^{3+}/Tb^{3+} phosphors can be well excited by 375 nm near UV wavelength.

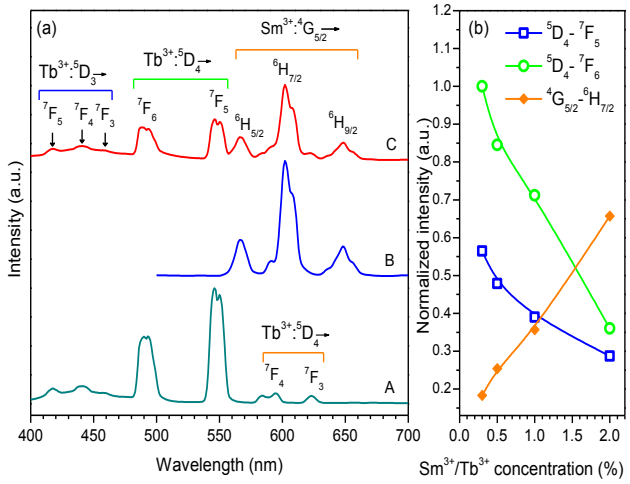

Fig. 6. PL spectra [(A) 0.5%Tb^{3+}, (B) 1%Sm^{3+}, (C) 2%Sm^{3+}/0.5%Tb^{3+}] for YAB:Sm^{3+}/Tb^{3+} phosphors under 375 nm near UV wavelength excitation (a) and the variation of intensity of prominent emission transitions with Sm^{3+}/Tb^{3+} concentration (b).

The evaluated CIE chromaticity coordinates are summarized in Table 1 and located in the CIE chromaticity diagram shown in Fig. 5. Upon 375 nm excitation, the YAB:0.5%Tb^{3+} phosphor emits green colour with CIE chromaticity coordinate (x = 0.283, y = 0.418) and the YAB:1%Sm^{3+} phosphor emits yellow colour with CIE chromaticity coordinate (x = 0.460, y = 0.475). On the other hand, the emission colour of Sm^{3+}/Tb^{3+} co-doped YAB phosphors can be tuned from green-to-white by modifying the Sm^{3+} concentration [green for 0.3% Sm^{3+}, greenish-white for 0.5% Sm^{3+}, yellowish-white for 1% Sm^{3+} and white for 2% Sm^{3+}]. The ($^4G_{5/2} \rightarrow {}^6H_{9/2}$ / $^4G_{5/2} \rightarrow {}^6H_{7/2}$) intensity ratio is also kept constant at around 0.24 (see Table 1) for 1%Sm^{3+}- and Sm^{3+}/Tb^{3+} co-doped YAB phosphors. The quite smaller and constant value of ($^4G_{5/2} \rightarrow {}^6H_{9/2}$ / $^4G_{5/2} \rightarrow {}^6H_{7/2}$) intensity ratio also supports that the Sm^{3+} and Tb^{3+} ions are embedded in the inversion symmetry sites of YAB lattice. Negligibly small variation in the average value of ($^4G_{5/2} \rightarrow {}^6H_{9/2}$ / $^4G_{5/2} \rightarrow {}^6H_{7/2}$) intensity ratio might be due to the experimental errors while recording the PL measurements. Though the concentration of Sm^{3+} ions is increased in YAB:*x*Sm^{3+}/0.5%Tb^{3+} phosphors, the emission transitions of Sm^{3+} ions are peaked at the same position and no significant change in the spectral widths is noticed under 406 and 375 nm excitations. These results indicate that there is no change in the structural environment around Sm^{3+} ions in YAB phosphor. Based on this discussion, we suggest that the Tb^{3+}-, Sm^{3+}- and Sm^{3+}/Tb^{3+} codoped YAB phosphors can be potential for SSL applications.

3.4. Luminescence decay

The luminescence decay of $^4G_{5/2}$ emission state of Sm^{3+} ion in YAB:Sm^{3+}/Tb^{3+} phosphors is studied by monitoring the emission at 602 nm and excitation wavelength at 406 nm. The normalized intensity verses time curves are described in Fig. 7. The decay curves are suitably fitted to single exponential function, $I = I_0\, e^{-t/\tau}$, here I is the intensity at time t, I_0 is the initial intensity when t = 0 and τ is the lifetime. The lifetime of an emitting level has been predicted by taking the first e-folding times of the intensity of decay curves. The lifetime of $^4G_{5/2}$ level in YAB:1%Sm^{3+} phosphor is 1.11 ms, where as in YAB:*x*Sm^{3+}/0.5%Tb^{3+} phosphors it is 1.23, 1.19, 1.15 and 1.09 ms for *x* = 0.3, 0.5, 1.0 and 2.0%, respectively. The gradual decrease in lifetime with the increase of Sm^{3+} concentration can be attributed to the increased interactions among the excited Sm^{3+} ions.

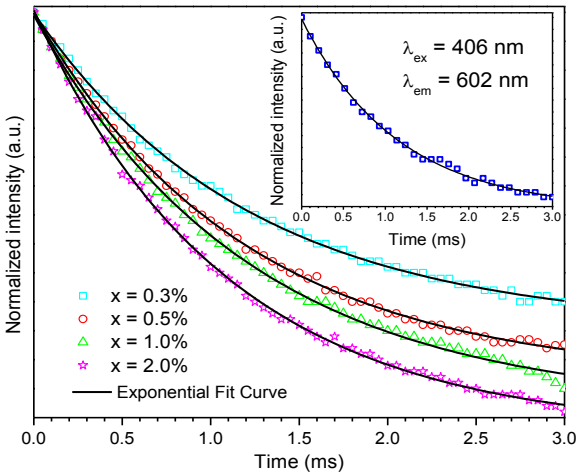

Fig. 7. Normalized decay curves of $^4G_{5/2}$ state of Sm^{3+} ion in YAB:xSm^{3+} / 0.5%Tb^{3+} phosphors. Inset shows the normalized decay profile for YAB:1%Sm^{3+} phosphor.

The luminescence decay profiles of $^5D_4$ emission state of Tb^{3+} ion in the presence and absence of Sm^{3+} ions in YAB phosphors (λ_{ex} = 375 nm and λ_{em} = 546 nm) are illustrated in Figs. 8a and b, respectively. These decay profiles are also well fitted to single exponential function mentioned above. The values of lifetime estimated by taking the first e-folding times of the intensity of decay curves are summarized in Table 2. The lifetime of $^5D_4$ (Tb^{3+}) decreases with the increase of Sm^{3+} concentration due to the ET from Tb^{3+} to Sm^{3+} ions. The variation of lifetime of $^5D_4$ (Tb^{3+}) level as a function of Sm^{3+}/Tb^{3+} concentration is presented in Fig. 8c.

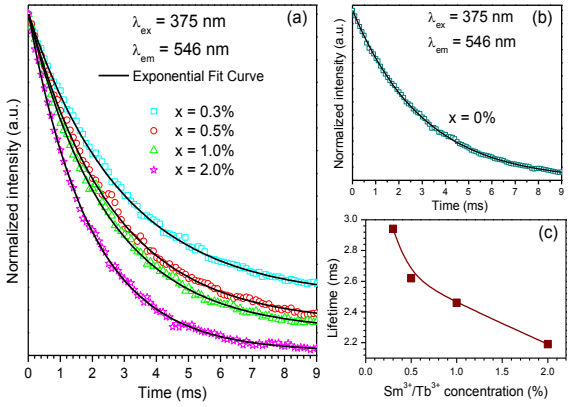

Fig. 8. Normalized decay curves of $^5D_4$ state of Tb^{3+} ion in YAB:xSm^{3+}/0.5%Tb^{3+} (a), YAB:0.5%Tb^{3+} (b) phosphors and the lifetime verses Sm^{3+} / Tb^{3+} concentration (c).

Table 2. Lifetime (τ) of $^5D_4$ (Tb^{3+}) emission level, energy transfer efficiency (η_{ET}) and energy transfer rate (ρ_{ET}) from Tb^{3+} to Sm^{3+} in YAB:xSm^{3+}/0.5%Tb^{3+} phosphors under 375 nm excitation.

Sm^{3+} concentration (x %)	τ (±0.20 ms)	η_{ET} (%)	ρ_{ET} (s^{-1})
x = 0	3.02	-	-
x = 0.3	2.94	2.65	9.01
x = 0.5	2.62	13.24	50.55
x = 1.0	2.46	18.54	75.38
x = 2.0	2.19	27.48	125.50

3.5. Energy transfer from Tb^{3+} to Sm^{3+}

In case of co-doping of RE ions, the luminescence quenching occurs due to the ET from donor ions to the acceptor ions until the energy sink is reached in the lattice and at critical concentration the average shortest distance between the nearest activator ions is equal to the critical distance [26]. The critical transfer distance (R_c) can be calculated using the formula:

$$R_c \approx 2\left(\frac{3V}{4\pi x_c N}\right)^{1/3} \quad (3)$$

where V is the volume of the unit cell, x_c is the total critical concentration of dopant ions when the luminescence intensity of sensitizer decreases to its half that in the sample in the absence of activators and N is the number of available crystallographic sites per unit cell. For YAB phosphors, N and V are 3 and 541.94 $Å^3$, respectively. In the present investigation, the value of x_c is 1.0% (0.5%Tb^{3+}+0.5%Sm^{3+}) and the critical transfer distance for efficient ET is estimated to be ~32.55 Å. The average distance (R_{ran}) between Tb^{3+} and Sm^{3+} ions has been determined assuming a random distribution of ions [27]:

$$R_{ran} = 2\left(\frac{3}{4\pi(C_{Tb}+C_{Sm})}\right)^{1/3} \quad (4)$$

where C_{Tb} and C_{Sm} are the total concentrations of Tb^{3+} and Sm^{3+} ions, respectively. The values of C_{Tb}, C_{Sm} and R_{ran} are 2.54×10^{19} ions/cm^3, 2.57×10^{19} ions/cm^3 and 33.43 Å, respectively. Here it is note-worthy that at total critical concentration, the average distance between Tb^{3+} and Sm^{3+} ions is slightly higher than the critical transfer distance which supports the formation of Sm^{3+}-Tb^{3+} clusters. Thus, an efficient ET from Tb^{3+} to Sm^{3+} takes place in YAB:xSm^{3+}/0.5%Tb^{3+} phosphors for x = 0.5, 1.0 and 2.0%. This can also be verified by evaluating the ET efficiency (η_{ET}) and the ET rate (ρ_{ET}) from the sensitizer (Tb^{3+}) to an activator (Sm^{3+}) using the lifetime of the emitting level of sensitizer. The values of η_{ET} and ρ_{ET} has been calculated using the following equations [28,29]:

$$\eta_{ET} = \left(1-\frac{\tau}{\tau_0}\right) \quad (5)$$

$$\rho_{ET} = \frac{\eta_{ET}}{(1-\eta_{ET})\tau_0} \quad (6)$$

where τ and τ_0 are the corresponding lifetimes of the sensitizer (Tb^{3+}) in the presence and absence of activator (Sm^{3+}) ion, respectively. The observed values of η_{ET} and ρ_{ET} for x = 0.5, 1.0 and 2.0% presented in Table 2 are evidence for an efficient ET from Tb^{3+} to Sm^{3+}. The type of electric multi-pole interaction (s) through which the ET from Tb^{3+} to Sm^{3+} ions take place has been estimated from the integrated intensity of Tb^{3+}:$^5D_4 \rightarrow {}^7F_5$ (546 nm) transition of YAB:xSm^{3+}/Tb^{3+} phosphors. According to Van Uitert [30], the relationship between the luminescence intensity of the donor ions (Tb^{3+}) and the concentration (C) of the acceptor ions (Sm^{3+}) satisfies the following equation:

$$\frac{I}{I_0} = (1+AC^{s/3})^{-1} \quad (7)$$

where I and I_0 are the luminescence intensity of donor ions (Tb^{3+}) in the presence and absence of acceptor ions (Sm^{3+}), respectively and A is a constant for the selected host and is independent of the doping concentration. The electric multi-pole interaction parameter (s) taking the values 3 for exchange, 6 for dipole-dipole, 8 for dipole-quadrupole, and 10 for quadrupole-quadrupole interactions can be calculated from the slop of $\log[I/I_{0(Tb)}]$ vs. $\log(C_{Sm})$ curve shown in Fig. 9. The slope parameter (s/3) can be calculated by fitting the experimental data to a linear equation: y = - (0.97±0.12) x - (2.24±0.23). From this equation, the value of s/3 is nearly equal to unity and the multi-pole interaction parameter (s) becomes 3. The estimated value of 's' evident that the transfer of energy from Tb^{3+} to Sm^{3+} is possible through the exchange interaction mechanism in Sm^{3+}-Tb^{3+} clusters instead of from these ions randomly distributed in YAB lattice. From the systematic investigation on PL and ET, we suggest that the Tb^{3+} ion acts as an efficient sensitizer of luminescence of Sm^{3+} in YAB host lattice and the YAB:Sm^{3+}/Tb^{3+} phosphors are promising materials for SSL devices.

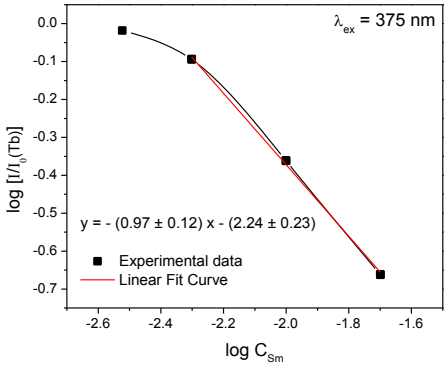

Fig. 9. Log [$I/I_{0(Tb)}$] verses log C_{Sm} plot for YAB:xSm^{3+}/Tb^{3+} phosphors.

4. Conclusions

Sm^{3+}/Tb^{3+} co-doped YAB phosphors were prepared by solid state reaction method and their phase, structural, optical and energy transfer studies were discussed in detail. The studied phosphor materials were crystallized in huntite type structure with space group R32 and indexed to JCPDS Card No. 72-1978. The average crystallite size of the YAB:Sm^{3+}/Tb^{3+} phosphors is estimated to be 54 and 55 nm from the Scherrer's and the Hall-Williamsons' methods, respectively. The YAB:Sm^{3+}/Tb^{3+} phosphors display the emission peaks in blue ($^5D_3 \rightarrow {}^7F_{5,4,3}$), green ($^5D_4 \rightarrow {}^7F_{6,5,4,3}$) and orange-red ($^4G_{5/2} \rightarrow {}^6H_{5/2,7/2,9/2}$) regions under an excitation wavelength of 375 nm. Almost constant spectral width of $^4G_{5/2} \rightarrow {}^6H_{5/2,7/2,9/2}$ transitions and the ($^4G_{5/2} \rightarrow {}^6H_{9/2}$ / $^4G_{5/2} \rightarrow {}^6H_{7/2}$) intensity ratio demonstrates that the Sm^{3+} and Tb^{3+} ions are located at the inversion symmetry sites of YAB lattice. The PL measurements reveal that the Tb^{3+} ion acts as an efficient sensitizer of luminescence of Sm^{3+} ions under 375 nm excitation. In case of Sm^{3+}/Tb^{3+} co-activated YAB phosphors, the Tb^{3+} ion induces the energy transfer from Tb^{3+} to Sm^{3+} through exchange interaction mechanism in Sm^{3+}-Tb^{3+} clusters only. Based on the experimental results, we suggest that the Tb^{3+}-, Sm^{3+}- and Sm^{3+}/Tb^{3+} codoped YAB phosphors can be potential for SSL devices.

Acknowledgements

One of the authors Dr. B.C. Jamalaiah would like to thank the Fundação para a Ciência e a Tecnologia (FCT), Ministério da Educação e Ciência, PORTUGAL for supporting him as a Post-Doctoral Researcher wide Ref. No. SFRH/BPD/76581/2011.

References

[1] E. Pavitra, G. Seeta Rama Raju, Yeong Hwan Ko, Jae Su Yu, Phys. Chem. Chem. Phys. **14**, 11296 (2012).
[2] Xiaoming Liu, Jun Lin, J. Mater. Chem. **18**, 221 (2008).
[3] G. V. Lokeswara Reddy, L. Rama Moorthy, B. C. Jamalaiah, T. Sasikala, Ceram. Int. **39**, 2675 (2013).
[4] Hyoung Sun Yoo, Won Bin Im, Jong Hyuk Kang, Duk Young Jeon, Opt. Mater. **31**, 131 (2008).
[5] Hua Yang, Zhouyun Ren, Yuming Cui, Lianxiang Yu, Shouhua Feng, J. Mater. Sci. **41**, 4133 (2006).
[6] Zhouyun Ren, Chunyan Tao, Hua Yang, J. Mater. Sci. Mater. Electron. **19**, 319 (2008).
[7] Jiayue Sun, Junhui Zeng, Yining Sun, Jicheng Zhu, Haiyan Du, Ceram. Int. **39**, 1097 (2013).
[8] Grazyna Dominiak-Dzik, J. Alloys Compd. **391**, 26 (2005).
[9] Jia Zhang, Yuhua Wang, Linna Guo, Yan Huang, J. Am. Ceram. Soc. **95**, 243 (2012).
[10] J. Madarasz, E. Beregi, J. Sztatisz, I. Földvari, G. Pokol, J. Therm. Anal. Calorim. **64**, 1059 (2001).
[11] L. J. Q. Maia, A. Ibanez, L. Ortega, V. R. Mastelaro, A. C. Hernandes, J. Nanopart. Res. **10**, 1251 (2008).
[12] Preetam Singh, Ashvani Kumar, Ajay Kaushal, Davinder Kaur, Ashis Pandey, R. N. Goyal, Bull. Mater. Sci. **31**, 573 (2008).
[13] Lin-Li Zhang, Chang-Xin Guo, Jun-Jing Zhao, Jun-Tao Hu, Chin. Phys. Lett. **22**, 1225 (2005).
[14] Yongchen Shang, Piaoping Yang, Wenxin Wang, Yanli Wang, Na Niu, Shili Gai, Jun Lin, J. Alloys Compd. **509**, 837 (2011).
[15] E. Beregi, A. Watterich, L. Kovacs, J. Madarasz, Vib. Spectrosc. **22**, 169 (2000).
[16] B. Yan, C. Wang, Solid State Sci. **10**, 82 (2008).
[17] P. Apte, H. Burke, H. Pickup, J. Mater. Res. **7**, 706 (1992).
[18] Z. Xu, J. Yang, Z. Hou, C. Li, C. Zhang, S. Huang, J. Lin, Mater. Res. Bull. **44,** 1850 (2009).
[19] Sun Hong-Tao, Zhang De-Bao, Xu Shi-Qing, Dai Shi-Xun, Hu Li-Li, Jiang Zhong-Hong, Chin. Phys. Lett. **21**, 1759 (2004).
[20] W. T. Carnall, P. R. Fields, K. Rajnak, J. Chem. Phys. **49**, 4424 (1968).
[21] Rik Van Deun, Koen Binnemans, C. Gorller-Walrand, Jean-Luc Adam, Proc. SPIE **3622**, 175 (1999).
[22] Richard K. Brow, David R. Tallant, Gary L. Turner, J. Amer. Ceram. Soc. **79**, 2410 (1996).
[23] W. T. Carnall, P. R. Fields, K. Rajnak, J. Chem. Phys. **49**, 4447 (1968).
[24] G. Lakshminarayana, R. Yang, J. R. Qiu, M. G. Brik, G. A. Kumar, I. V. Kityk, J. Phys. D: Appl. Phys. **42**, 015414 (2009).
[25] Rong Wang, Jin Xu, Chao Chen, Mater. Lett. **68**, 307 (2012).
[26] G. Blasse, Phys. Lett. A **28**, 444 (1968).
[27] R. Martínez-Martínez, M. García, A. Speghini, M. Bettinelli, C. Falcony, U. Caldiño, J. Phys.:Condens. Matter **20**, 395205 (2008).
[28] P. I. Paulose, G. Jose, V. Thomas, N. V. Unnikrishnan, M. K. R. Warrier, J. Phys. Chem. Solids **64**, 841 (2003).
[29] U. Caldiño, J. L. Hernández-Pozos, C. Flores, A. Speghini, M. Bettinelli, J. Phys.: Condens. Matter **17**, 7297 (2005).
[30] L. G. Van Uitert, J. Electrochem. Soc. **114**, 1048 (1967).

*Corresponding author: bcjamal@hotmail.com